Sindh Univ. Res. Jour. (Sci. Ser.) Vol.47 (2): 367-370 *(2015)*

SINDH UNIVERSITY RESEARCH JOURNAL (SCIENCE SERIES)

Computation of Wall Shear Stresses Across Various Stenosis Length in Common Carotid Artery

A. A. SHAIKH[+], F. H. CHANDIO* , S. QURESHI

Department BSRS, Mehran University of Engineering & Technology, Jamshoro

Received 21st February 2015 and Revised 08th June 2015

Abstract: The main focus of this article is specified on laminar flow simulation in large stenosed arteries is in which the important factor of wall shear stresses is explored across various stenosis length ratio (*L/D*) varied from 10 to 40.The results of various stenosis lengths are compared with various degrees of stenosis (*d/D*) ranging from 20% to 80% at different Reynold numbers i.e. R*e* = 500 and R*e* =1000. The computational simulation is carried out under axisymmetric steady laminar flow on stenosis ranging from 20% to 80% at selected R*e* numbers of 500 and 1000. The effects of Reynold numbers on shear stresses and also stenosis length on wall shear rate are highlighted in details. To avoid from any divergence, numerical calculations are performed up to Reynolds number of 1000. Semi Implicit pressure correction Scheme and Finite Element Method (FEM) is used to solve the Navier-Stokes equations for viscous flow.

Keywords: Finite element, Common Carotid Artery, laminar Blood flow, Stenosis

1. INTRODUCTION

So many abstract and untried studies have been discussed / investigated to understanding the pattern of flow disorders in the presence of stenosis. Deplano and Siouffi (1999) discovered the models for stenosis using mathematically and Doppler ultrasonic velocimeter . In their reports they have analyzed that the factor of velocity field is extremely reliant on flow wave style especially at the downstream of the stenosis. Pulsatile blood flow in three axis symmetric as well as three symmetrical stenosed tube model have been discussed by Long *et al.* (2001) at different sizes of stenosis sternness. For all models the main attention is given on the zone of flow separation and the circulations of wall shear stress. Liao *et al.* (2004), Toufique Hasan and Dipak Kanti, (2008) explored the effect of narrowing ratio of stenosis, Womerssley number and Reynolds number on flow performance through stenosed arteries . In their research work they have ignored property of blood as non-Newtonian. Both Experimental and numerical methods have been employed by various researchers to determine the development of stenosis and its magnitude .They mainly focused upon computing shear stresses using different Reynolds numbers at variable obstruction sizes in the stenosed carotid arteries. Tu and Deville (1992) computed the flow of blood through stenosis by considering the property of blood as non –Newtonian by means of Herschel–Bulkley, Bingham and power-law fluids in a rigid circular tube with a fractional blocking. In their reports they have claimed that especially for severe stenosis, turbulences are robust by their vorticity intensity and continue after the geometrical hurdle. Carreau and Power law models are compared for 45% stenosis with trapezoidal profile by Chan *et al.* (2007) and concluded that Carreau model has little difference in terms of velocity , pressure and WSS where as more significant vortices and smaller WSS are observed in Power law model. Sankar and Lee (2009) used to solve herschel-bulkley model for flow of minor stenosis. In their conclusion they described that, with the rise of yield stress/pressure or stenosis tallness, the plug core radius, pressure drop and wall shear stress rise. The Casson fluid flow through a stenosed bifurcated artery has been investigated by Shaw *et al.* (2009), they concluded that for the femoral and coronary arteries difference of axial velocity and flow rate with yield stress is unchanging.

2. GEOMETRY AND BOUNDARY CONDITIONS

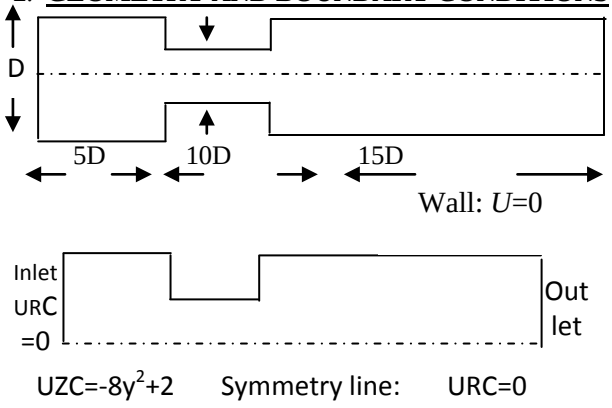

Fig. 1. Geometry of an arterial segment with a d% local stenosis and boundary conditions.

The no-slip boundary conditions were imposed on the wall as follows

[+]Corresponding Author: Email : asifali_1968@hotmail.com

*Institute of Mathematics and Computer Science , University of Sindh, Jamshoro.

$v_r = v_z = 0$ at $r = r_o(z)$

where $r_o(z)$ describes the local wall radius as a function of z. Total 6 nodes triangular elements are used with fine meshes near the walls along the stenosed region.

3. GOVERNING EQUATIONS

The continuity and Navier-Stokes equations are used in vector and component form for the axisymmetric confined flow of an incompressible fluid as below:

$$\frac{\partial u}{\partial x}+\frac{\partial v}{\partial y}+\frac{\partial w}{\partial z}=0$$

$$i-e\ \ \nabla.u=0 \qquad (1)$$

$$\rho_0\left(\frac{\partial u}{\partial t}+(u.\nabla)u\right)=-\bar{\nabla}p+\mu div\left(\nabla u\right)+\rho_0\bar{B} \qquad (2)$$

and in component form:

$$\frac{\partial v_r}{\partial r}+\frac{\partial v_z}{\partial z}+\frac{v_r}{r}=0$$

$$V_r\frac{\partial v_r}{\partial r}+V_z\frac{\partial v_r}{\partial z}=-\frac{1}{\rho}\frac{\partial p}{\partial r}+\mu\left[\frac{\partial^2 v_r}{\partial r^2}+\frac{1}{r}\frac{\partial v_r}{\partial r}-\frac{v_r}{r^2}+\frac{\partial^2 v_r}{\partial r^2}\right]$$

$$V_r\frac{\partial v_z}{\partial z}+V_z\frac{\partial v_z}{\partial z}=-\frac{1}{\rho}\frac{\partial p}{\partial z}+\mu\left[\frac{\partial^2 v_z}{\partial r^2}+\frac{1}{r}\frac{\partial v_z}{\partial r}+\frac{\partial^2 v_z}{\partial z^2}\right] \qquad (3)$$

Here physical coordinates r and z are located with z-axis on the symmetrical axis of the artery. No secondary or swirling flows are considered; therefore, v_r and v_z are the radial and axial components and are used for the total velocity , respectively. The pressure, density and kinematic viscosity are denoted by p, ρ, and μ, respectively. The situations at a large distance upstream and downstream of the stenosis are presumed to correspond to Poiseuille flow through a long, circular artery with a constant cross-section and their calculations are debated as:

$$v_z=U\left[1-\left(\frac{r}{D}\right)^2\right]$$

vr= 0 (4)

where U is the extreme velocity of the parabolic profile and D is the diameter of the artery in the blocked portion.

Characteristic scale D and a characteristic velocity scale U are used on The Navier-Stokes and continuity equations for non-dimensionalization to get:

Div u*= 0

$$\left(u^*.\nabla\right)=-\nabla p^*+\frac{1}{\mathrm{Re}}\nabla^2 u^* \qquad (5)$$

where u* and p* are dimensionless values for the velocity and pressure, respectively.

Non-dimensional variables are defined as

$$r^*=\frac{r}{D};\ z^*=\frac{z}{D};\ v_r^*=\frac{v_r}{U};\ \text{and}\ v_z^*=\frac{v_z}{U} \qquad (6)$$

where the non-dimensional Reynold number, Re, is defined as $\mathrm{Re}=\frac{\rho UD}{\mu}$.

Numerical Computations

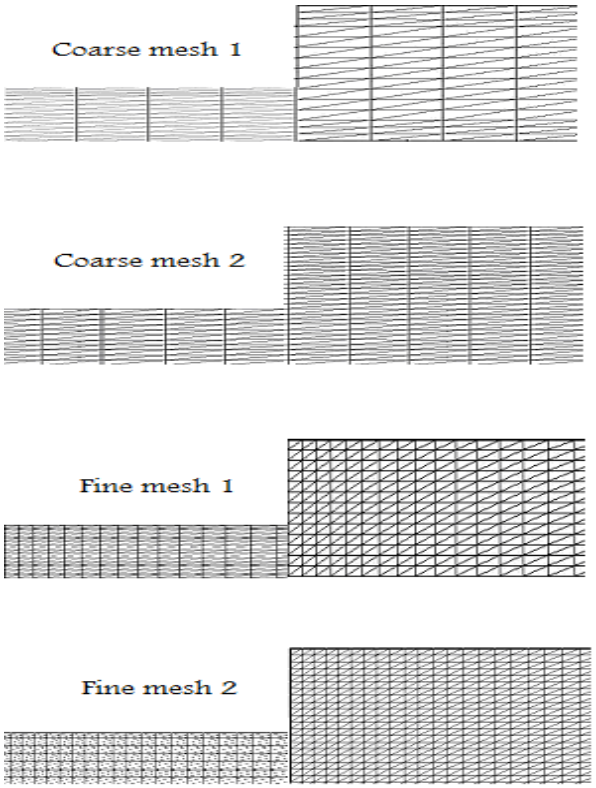

Fig. 2. The finite element meshes around 80% stenosis. Top to bottom are shown coarse mesh1, coarse mesh2, Fine mesh1 and Fine mesh2.

Grid dependence tests are performed on 80% stenosis with five grids downstream of the stenosis height, consisting of coarse mesh1, coarse mesh2, dense mesh1 and dense mesh2 having 1×8×16, 1×16×16, 2×8×16 and 2×16×16, elements respectively.

4. WALL SHEAR STRESS

A significant factor in arterial stenosis is the shear stress at the wall of the artery. **(Fig. 3)** shows the wall shear rate distribution as a function of distance from the origin of the stenosis with various constrictions (d/D) at a Re of 500. The highest and lowest absolute values in

wall shear rate appeared near the axial location of the vortex center and at the reattachment point, respectively. In the vortex region, the wall shear rates produced negative values, indicating that wall shear stresses were acting in different directions on both sides of the reattachment point.

The effects of Reynold number verses shear stresses and also effects of stenosis length verses shear stresses are described in details here.When the Reynolds number increased from 500 to 1000, the highest wall shear rate doubled accordingly **(Fig. 4).**

It has also been noticed that the stenosis length did not affect the wall shear rate distribution **(Fig. 5).** In this severe stenosis, the absolute value of the wall shear rate remained higher in the vortex than downstream point and these high stresses generates problems in the smooth flow of blood.

Downstream of the reattachment point, the wall shear rate approached the value found in a fully developed Poiseuille flow. When the stenosis was not severe, the absolute value of the wall shear rate remained lower in the vortex than in the fully developed Poiseuille flow.

Further it has been observed from the computational results that high wall shear rates are developed in the vortex region than it was downstream of the reattachment point

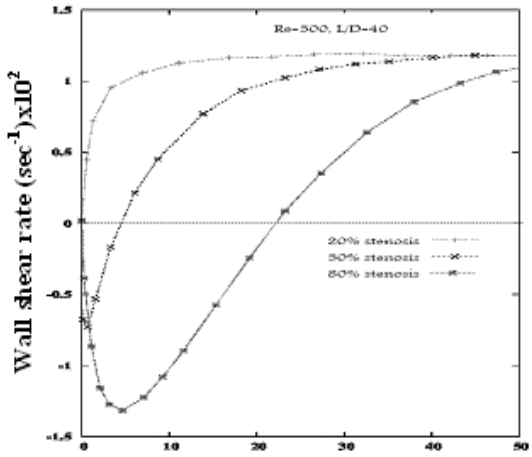

Fig.3. Wall shear rate plot as a function of the normalized axial distance from the stenosis. with various degrees of stenosis (d/D) at Re = 500.

However, at a constriction (d/D) of 0.5 (80% stenosis), the wall shear rates was higher in the vortex region than it was downstream of the reattachment point.

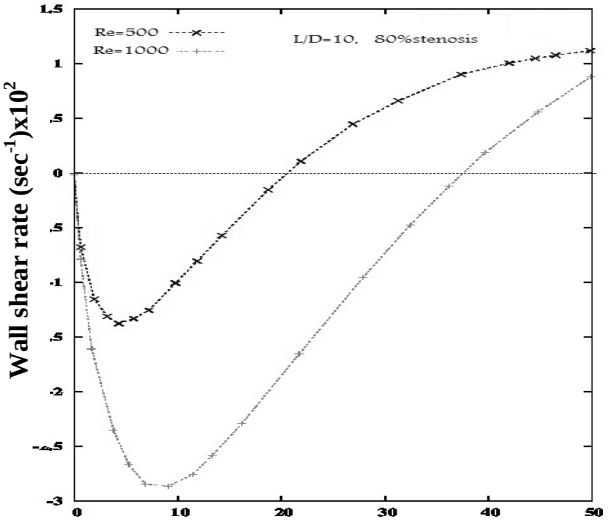

Fig.4. Wall shear rate plot as a function of the normalized axial distance from the stenosis. Effect of the Reynolds number on all shear rate distal to 80% stenosis degree (d/D) of 0.5.

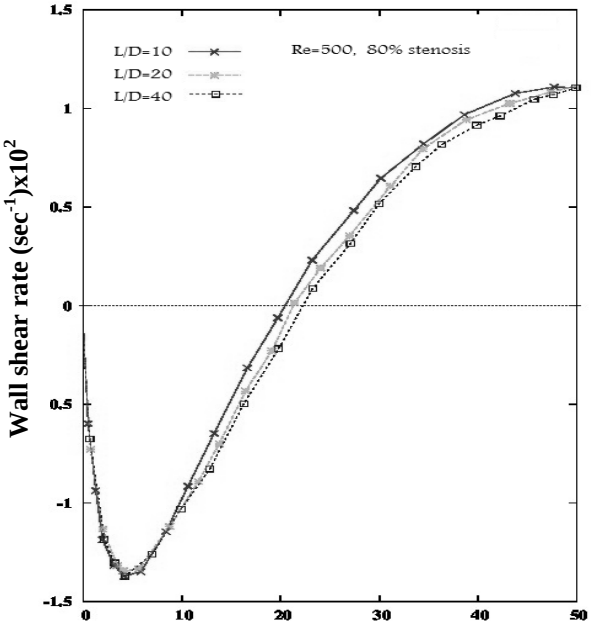

Fig. 5. Wall shear rate plot as a function of the normalized axial distance from the stenosis. Effect of stenosis Length on wall shear rate is given distal to 80% stenosis degree (d/D) of 0.5 and Re = 500.

5. RESULTS

Simulation of blood flow past various degrees of stenosis i-e d/D=20%, d/D=30% and d/D=80% at different stenosis length i-e L/D=10, L/D =20 and L/D =40 40 is deliberated in detail in this article. For the simulation, coarse and fine meshes are used to get the better accuracy of the results, the mesh sizes are taken as 1x8x16, 1x16x16, 2x8x16and 2x16x16, however computational results are performed for the size of mesh

2x16x16 with 18800 elements. The results performed through Simulation indicate that, at a constriction (d/D) of 0.5 (80% stenosis), the wall shear rates was higher in the vortex region than it was downstream of the reattachment point. When the Reynolds number enlarged from 500 to 1000, the highest wall shear rate doubled accordingly (Figure 4). Figure 5 presents a comparison of wall shear rates for various stenosis lengths (L/D) =10. (L/D)= 20, (L/D) =40 at Re=500 and stenosis degree i-e d/D = 0.5 (80% stenosis), indicating that the stenosis length did not disturb the wall shear rate circulation.

6. CONCLUSION

In this article computational results are highlighted by using different sizes of meshes i-e 1x8x16, 1x16x16, 2x8x16 and 2x16x16 at different degrees of stenosis i-e 20, 50 and 80 percentages. At these degrees of stenosis, the different lengths and also different Reynold numbers are also taken to analyses the flow pattern of blood and the complications during flow. The results are compared on the basis of (i) size of stenosis (ii) degrees verses Reynold number (iii) degree verses lengths. During this computation it is observed that high shear rate are noticed in vortex region for the stenosis of size 80%, also it has been observed that as the Reynold number increases then shear rates are also increasing and further it has been noticed during the computation that the shear rates are doubled as the Reynold number increases from 500 to 1000. Moreover it is also detected that length of stenosis did not make any disorder during the flow of blood

In the current study, it has been observed that absolute values of wall shear rates were small at the location of vortex for the slight size of stenosis i-e (20%), however it was noticed that the trend of wall shear stresses was increasing as the size of stenosis was increasing. In the severe stenosis (80% stenosis), the absolute value of wall shear rate remained higher in the vortex than downstream point which is dangerous for the smooth flow of blood which ultimately will be harmful for the health.

REFERENCES:

Chan, W.Y., Y. Ding, and J.Y. Tu, (2007), Modeling of non-Newtonian blood flow through a stenosed artery incorporating fluid–structure interaction. ANZIAM Journal 47 (EMAC2005), C507–C523.

Deplano, V., and M. Siouffi, (1999), Experimental and numerical study of pulsatile flows through stenosis: wall shear stress analysis. Journal of Biomechanics 32, 2081Pp.

Long, Q., X.Y. Xu, K.V. Ramnarine, and P. Hoskins, (2001) Numerical investigation of physiologically realistic pulsatile flow through arterial stenosis. Journal of Biomechanics 34, 1229–1242.

Liao, W., Lee, T.S., and Low, H.T. (2004), Numerical studies of physiological pulsatile flow through constricted tube. International Journal of Numerical Methods for Heat & Fluid Flow 14 (Iss: 5), 689–713.

Sankar, D.S., and U. Lee, (2009) Mathematical modeling of pulsatile flow of non-Newtonian fluid in stenosed arteries. Communications in Nonlinear Science and Numerical Simulation 14 (7), 2971–2981.

Shaw, S., R.S.R. Gorla, P.V.S.N., Murthy, and C.O. Ng, (2009), Pulsatile Casson fluid flow through a stenosed bifurcated artery. International Journal of Fluid Mechanics Research 36 (1), 43–63.

Toufique H. A.B.M., and D. K. Das. (2008) Numerical simulation of sinusoidal fluctuated pulsatile laminar flow through stenotic artery. Journal of Applied Fluid Mechanics 1 (2), .25–35.

Tu C., and M.Deville (1992) Finite element simulation of pulsatile flow through arterial stenosis, J. Biomech., Vol. 85, No. 10, 1141-1152.